PARTICLE SIZE REDUCTION IN DEBRIS FLOWS: LABORATORY EXPERIMENTS COMPARED TO FIELD DATA FROM INYO CREEK, CA

A thesis submitted to the faculty of
San Francisco State University
In partial fulfillment of
The requirement for
The degree

Master of Science
In
Geosciences

by

Omid Arabnia

San Francisco, California

May 2015

CERTIFICATION OF APPROVAL

I certify that I have read *Particle Size Reduction In Debris Flows: Laboratory Experiments Compared to Field Data from Inyo Creek, CA* by Omid Arabnia, and that in my opinion this work meets the criteria for approving a thesis submitted in partial fulfillment of the requirements for the degree: Master of Science in Geosciences at San Francisco State University.

Leonard Sklar
Professor of Earth and Climate Sciences

Jason Gurdak
Assistant Professor of Earth and Climate Sciences

Jerry Davis
Professor of Geography and Environmental Sciences

PARTICLE SIZE REDUCTION IN DEBRIS FLOWS: LABORATORY EXPERIMENTS COMPARED TO FIELD DATA FROM INYO CREEK, CA.

Omid Arabnia
San Francisco State University
2015

Rock particles in debris flows are reduced in size through abrasion and fragmentation. Wear of coarse sediments results in production of finer particles, which can alter the bulk material rheology influencing runout distance. Particle wear also affects the size distribution on hillslopes before delivering the sediment to the fluvial channel network. A better understanding of the controls on particle wear in debris flows is needed to infer flow conditions from debris flow deposits, estimate the initial size of sediments entrained in the flow, model debris flow dynamics, and map hazards. I used three rotating drums to create laboratory debris flows across a range of scales. Drum diameters range from 0.2 to 4.0 m, with the largest drum able to accommodate up to 2 Mg of debris, including boulders. I began the experiments with well-sorted, angular coarse particles, which evolved through particle wear in transport. The fluid was initially clear water, which rapidly acquired fine-grained wear products. After each 0.25 km of tangential travel distance, I quantified the particle size distribution. I calculated particle wear rates by fitting the Sternberg equation to the statistics of particle size and mass distributions. Mass wear rates are 2.9, 4.9. and 11%/km in the small, medium, and large drum, respectively. Rates of coarse particle wear and production of fragments and fine particles scale with the rate of energy expenditure per unit bed area, or unit drum power. I use this power scaling to estimate a mass particle breakdown rate of 13%/km at Inyo Creek, CA.

I certify that the Abstract is a correct representation of the content of this thesis.

Chair, Thesis Committee

May 18, 2015
Date

ACKNOWLEDGMENTS

I would like to thank Leonard Sklar for offering inspiration and optimism from the start. I never thought the process of earning a Master's degree could be so demanding, but lack stress. He is a true role model in all aspects of life and I feel so lucky to have worked with him! I would also like to thank Alexander Stuart Foster for his wizardry in the laboratory. This project would have had more limitations and ultimately be different without his assistance. I would also like to thank my committee members Jason Gurdak and Jerry Davis for all of their insight. A special thanks goes to my family, who made this journey possible! I don't even want to speculate my circumstances without such amazing people. Lastly, a special thanks goes out to my partner in crime, Gabriela, for the unwavering love and patience that makes every day beautiful and exciting.

Partial funding for this research was provided by the National Science Foundation. This money made for an amazing field experience that I will never forget. I would also love to thank David Dawdy for offering additional assistance. His generosity added a valuable chapter to my thesis that tightened up loose ends. His many stories stimulate, excite, and reassure me that this is the place for me.

TABLE OF CONTENTS

LIST OF TABLES

LIST OF FIGURES

1.0 Introduction

Debris flows and granular rock avalanches are a significant hazard in mountain landscapes, even at large distances downstream of sediment source areas because they can easily liquefy after initiation [Iverson, 2013]. Debris flow run-out distance is influenced by the particle size distribution (PSD) of the entrained sediment, particularly by the concentration of fine-grained sediments within the fluid matrix [Bowman et al., 2012; Iverson et al., 2010]. At least 3% by weight mud needs to be present in order to have pore pressures high enough to transition from granular rock avalanches (GRA) to debris flow motion [Iverson and George, 2014]. Therefore, GRAs can transition into debris flows after initiation if enough fine sediment is produced or entrained into suspension. PSDs evolve during transport due to particle abrasion and fragmentation, and due to entrainment and deposition of particles along the flow boundary. Although understanding the evolution of particle size distributions during granular rock avalanche and debris flow transport is important for hazard prediction and landscape evolution models, few data are available to guide modeling.

PSDs of fluvial networks, however, have concerned geologists for years due to their important role in fluvial landscape evolution. Most fluvial sediments fine downstream through channel networks [Kodama, 1994; Brierley and Hicken, 1985; Brewer and Lewin, 1993]. Sternberg (1875) proposed a one parameter model describing the fining of sediment in fluvial channels as:

$$D = D_0 e^{-\alpha_D x} \qquad [1]$$

where D is grain size [L], x is distance traveled [L], D_0 is initial grain size [L], and α_D is the abrasion coefficient [(L/L)/L]. This functional form can also be used to quantify the mass loss with distance:

$$M = M_0 e^{-\alpha_M x} \qquad [2]$$

where M is the mass of a single particle or the bulk mass of coarse particles [M], and M_0 is the initial mass of the particle or particles [M]. Due to the differences between fluvial environments and GRA/debris flow environments, it is unclear whether equations 1 and 2 can be applied to GRA/debris flow areas. Debris flows exhibit a curved signature on log-log area-slope plots, and fluvial environments exhibit a log-linear trend [Stock & Dietrich, 2003]. Debris flows and GRAs are dominant in high slope areas with small drainage areas, and the opposite is true for fluvial channels. Debris flows and GRAs have more energetic particle interactions and higher degrees of fragmentation than fluvial environments.

Particle wear rates should depend on the intensity of particle interactions and on rock properties controlling resistance to wear. The intensity of the interactions changes with the rheology and pore pressures inside the flow. The runout distance and speed of debris flows are a function of the pore pressure [Iverson, 2013]. Pore pressure inside the flow is partly a function of the PSD. Understanding PSD evolution will be instrumental in modeling the pore pressure evolution to better understand runout distance and map hazardous areas.

The episodic and violent nature of debris flows and GRAs makes them difficult to study in natural environments. Therefore, experimental studies can provide essential data. Previous experiments on debris flows have used planar chutes of limited length [e.g. Iverson et al., 2010], and rotating drums [Hsu et al., 2008, Hsu et al., 2014; Schneider et al., 2011; Kaitna et al., 2014], which permit longer transport distances. Mass abrasion rate in drum transport can be measured by weighing the particles before and after tumbling to calculate the fraction of the mass lost to silt, and dividing this amount by distance traveled. For a given rock type, abrasion rates are a function of the particle interactions inside the drum, which depend on the details of the experimental set up (i.e. drum radius, rotation speed, water content, sediment size and concentration, etc.). As a result, it remains unclear how to scale abrasion rates, and the evolution of PSDs, measured in a laboratory drum experiments, to a field setting.

To address this critical knowledge gap I used three drums of differing sizes to determine the effect of drum size on particle abrasion and fragmentation rates in experimental debris flows (Figure 1). Our goal is to develop a method for scaling between laboratory drums and field settings, which can be used to predict the evolution of coarse PSDs and production of fine sediment added to the fluid phase of a natural debris flow that presumably initiated as a GRA at Inyo Creek in the southeastern Sierra Nevada range of California (Figure 2).

2.0 Experimental Methods

2.1 Experimental set-up and scaling

I used three drums with diameters ranging from 0.20 to 4.0 meters (Figure 1), located at University of California, Berkeley's Richmond Field Station laboratory, to study the evolution of PSDs as a function of travel distance and drum diameter. The two largest devices have been used previously to study debris flow dynamics and bedrock erosion [Hsu et al., 2008, Hsu et al., 2014; Schneider et al., 2011; Kaitna et al., 2014]. The drum beds contain vanes perpendicular to the flow to inhibit sliding and promote development of a shear layer. Shear rate varies with rotational velocity, which can be adjusted with variable speed controllers that control the motor speed.

The drum and sediment dimensions are scaled to maintain geometric similarity across drum sizes; drum radius is thus the independent factor that all other spatial variables are scaled by (Tables 1 and 2). For example, flow width is 40% of drum radius. The initial median particle size was selected so that the ratio of drum width to particle diameter was at least 7.0 to prevent cross-flow bridging. Similarly, the initial volume of sediments was selected so that the flow depth was equal to at least 6 particle diameters to create a shear layer within the flow.

Following Schneider et al. [2011], I used the rotational Froude number (Fr) to maintain dynamic similarity between drums. The rotational Froude number quantifies the ratio of the centripetal acceleration to the gravitational acceleration and is equal to:

$$F_r = \omega^2 \frac{r}{g} \quad [3]$$

where ω is the angular velocity of the drum [1/T], r is drum radius [L], and g is acceleration due to gravity [L/T^2]. I adjusted the velocity to maintain Fr = 0.05, to minimize centripetal acceleration while providing sufficient collisional energy to produce measurable abrasion in reasonable time. This led to tangential drum speeds of 1, 0.37, and 0.23 m/s in the 4, 0.56, and 0.2 m drums, respectively. The centripetal acceleration is equal to:

$$a_c = \frac{u_T^2}{r} \quad [4]$$

where u_T is the tangential velocity of the drum [L/T], and r is the drum radius [L]. This led to the drums having centripetal accelerations equal to ~ 0.5 m/s^2. Therefore, centripetal acceleration was only 5% of the gravitational acceleration.

Collisional energy can be characterized by the Savage number (Ns). The Savage number quantifies the ratio of grain collision stress to bulk intergranular stress caused by gravity, and can be written as:

$$N_s = \frac{\rho_s D^2 (\partial u/\partial z)^2}{(\rho_s - \rho_f) gh} \quad [5]$$

where $\partial u/\partial z$ is the shear rate [(L/T)/L], ρ_s and ρ_f are the solid and fluid densities respectively [M/L^3], and h is the thickness of the flow [L]. The scaling choices described above result in $N_s \sim 0.03$ in all drums.

Although F_r and N_s are constant across drums, the absolute magnitude of energy expended in during transport varies considerably between drums. Energy expenditure can be compared across drums using unit drum power (W/m^2), which I calculate as:

$$\frac{\Omega}{A} = \frac{\rho_b r u_T g S}{12} \tag{6}$$

where Ω is power [ML^2/T ^{3}], A is unit bed area [L^2], ρ_b is bulk density [M/L^3], u_T is tangential velocity [L/T], and S is flow surface slope [L/L]. Surface slope was determined by analyzing photographs taken through acrylic windows while the drum was in motion.

I obtained granodiorite clasts of various sizes from the GraniteRock Quarry in Aromas, CA, and used the Brazilian Test to obtain a tensile strength estimate of 7.6 MPa (Figure 3). The rocks for the 4 m drum were chosen by hand with a group of 3 volunteers because the quarry did not have the size class necessary separated out. The size classes needed in the other devices were purchased in bulk, and sorted out at the laboratory in order to create the scaled down PSD. Other variables and their values in the experimental setup are given in Table 1 and 2.

2.2 Experimental procedure and measurements

Each set of experimental runs began with a unimodal size distribution of fresh angular rock particles and clear water (Figure 4). Therefore, initially, the flows are GRAs. After 250 m of tangential travel distance, all particles and water were removed from the drum for measurement. Afterward, all sediments and water were placed back into the drum and tumbled for another 250 m. The experiment concluded after 1 km of travel distance, for a total of four runs in each drum

In the 4 m drum experiment, I measured the a, b, and c axes with calipers, and the weight of all particles with b-axis > 19 mm; all smaller particles were sieved. A crew of 3 people on calipers and one data logger were necessary to finish the set of runs in the device within several months. About 10 helpers would rotate into the positions throughout the months. The high financial cost, as well as the amount of time necessary to complete this type of analysis, led to us to develop a sampling technique which I then implemented in the 0.56 m drum experiment. All particles larger or equal to 0.3 g were weighed individually. Caliper measurements were done on a random 10% of this population. The population was chosen by first choosing a particle from the whole population and then drawing a playing card from a full deck. If the card was an ace, it was included in the sample population. Therefore, there were 1:13 odds of drawing a rock that would be included in the sample population. Particles larger than 2.8 mm and less than 0.3 g were sieved and counted and the rest of the particles were only sieved. In the 0.20 m drum, I weighed all particles initially and after 1 km of travel. In addition, after each 0.25 km run, I used a 2 mm sieve to separate the sediments and weighed the bulk mass of all particles not passing through the sieve. In all three drums, the water was sampled between runs and the suspended sediments were filtered, dried, and weighed.

3.0 Field site and methods

My goal is to predict breakdown and fragmentation rates at Inyo Creek, which is located in the Southeastern Sierras by Lone Pine, CA (Figures 2 & 3). This channel has a relief of 2 km in 3 km of longitudinal distance. Due to very steep granodiorite slopes, debris flows and GRAs are frequent here. In July of 2013, a significant debris flow occurred here. In the summer of 2014, abundant evidence remained for reconstructing flow surface elevations. In one bend I observed superelevation of high flow lines on the outer bank, relative to the inner bank, providing an opportunity to reconstruct the bulk flow dynamics. The height of the superelevation can be used to estimate mean velocity of the flow [Chow 1959, Pierson and Costa, 1987]. The height difference between banks correlates to the mean velocity of the flow around the bend using the following formula:

$$u = \left(\frac{R_C g cos(\theta_C)}{B}\Delta h\right)^{0.5} [\left(\frac{R_C}{h}\right)^{0.73}\left(\frac{\Delta h}{B}\right)^{0.73} 4.4^{-1.23}] \qquad [7]$$

where u is the mean flow velocity [L/T], Rc is the radius of curvature of the bend [L], g is gravitational acceleration [L/T^2], θc is the channel slope [L/L], B is channel width [L], h is the flow height [L], and Δh is the height difference of the two banks [L] (Figure 12) [Scheidl et al, 2015]. I used a total station to survey the flow path center line, high flow bank elevations, and a sequence of 6 cross sections at Inyo Creek. These surveys were used to calculate all the variables necessary in equation 7.

I collected PSD of debris flow deposits at 6 sites covering 1 km of relief (Figure 5). PSD were collected by photo sieving (Figure 6) [Bunte & Abt, 2001]. Photo transects were taken parallel and perpendicular to the flow direction at all sites except the highest elevation site. Stream width was too small to do a cross stream profiles at this location. The GPS coordinates of the transect endpoints were recorded and later put into GIS. Cross stream transects started and stopped at the edge of the debris flow deposits. The parallel to flow transects typically covered as much of the reach as possible, starting and stopping where slopes were low enough in the channel to survey. Images were then imported into ImageJ, where the b-axis of particles was collected along the transect. Clasts were measured every 0.1 m. Particles as small as 4 cm could be measured using this method. This method underestimates the PSD because the photos are of particles in their natural orientation, which may partially bury or hide it from view. This method was advantageous because I could use my time in the field to take photos and do the analysis at home. This leads to a much larger data set than if I had done pebble counts in the field.

To scale between the laboratory and field site I use power per unit bed area, which for the field case can be calculated as:

$$\frac{\Omega}{A} = \rho_b g h u S \qquad [8]$$

where ρ_b is bulk density [M/L^3], h is mean flow depth [L], u is flow velocity [L/T], and S is reach-averaged channel gradient [L/L]. The velocity calculated with equation 7 is used in equation 8.

4.0 Experimental Results

4.1 Evolution of particle size distributions

Particle size distributions became finer over the 1 km travel distance in each of the three drums, due to both abrasive wear that produced sand and silt, and fragmentation that produced gravel-sized particles. Figure 4 shows the measured PSDs for each experiment. For the experiments in the 4.0 and 0.56 m diameter drums, I separate the size distributions of the 1391 'original' particles, and the 'new fragments', using the assumption that no newly formed fragments are larger than any of the remaining original particles. The smallest drum did not form new fragments. Comparing the full distributions (Figs 4a, 4c, 4e) and the split distributions (Figs 4b and 4d), demonstrates that overall fining is due to both abrasion and fragmentation.

Figure 7 shows the evolution with travel distance in the characteristic percentiles of the full distributions, the D16, D50 and D84, in each experiment. For each percentile I quantified the rate of fining by fitting the exponential fining coefficient in equation 1. Comparing drums, I find that fining coefficients are greatest for the large drum (4.0 m), but surprisingly, the small drum (0.2 m) produced higher fining coefficients than the medium-sized drum (0.56 m). In each experiment, the fining coefficients are greatest for the D16 and least for D84.

4.2 Mass loss from gravel and coarser particles

I use equation 2 to quantify the mass lost from the coarse size-fraction ($D > 2$ mm and $D > 250$ microns) by production of sand and silt by abrasion. Although the mass of fine sediments remains within the debris flow, I consider production of fine sediments a mass transfer from the solid to the fluid phase of the flow. Figure 8 shows the change in mass fraction of the particles greater than 2 mm with travel distance for the three experiments; best-fit mass loss coefficients range from 0.029/km for the small drum to 0.11/km for the large drum.

Figure 9 shows the production of sediment smaller than 250 microns. This is the smallest mutual size sieved in all experiments. The best-fit mass loss coefficients in this case range from 0.004/km for the small drum to 0.061/km for the large drum. Taking 3% as the threshold concentration of fine sediment needed to create high enough pore pressures to transition from a GRA to a debris flow, only the largest scale experiment evolved from a GRA into a debris flow.

4.3 Production of new coarse particles

Because I hand-measured individual particles, I was able to document the rate that new coarse particles were produced by fragmentation. To be consistent with the geometric scaling between drums, I calculated fragment production as the number of new clasts larger than a threshold size, which was scaled by the radius of the drum (1.0, 2.8, 19.0 mm in the 0.20 m, 0.56 m, and 4 m drums respectively). As shown in Figure 9a, fragment production in the large drum was an order of a magnitude larger than in the medium drum at each 0.25 km increment of travel distance. Production in the small drum was negligible. Although production of coarse fragments was most rapid in the large drum, the mass of those new fragments was small compared with the mass of sand and silt generated by abrasion and fragmentation combined. This is shown in Figure 9b, where the mass eroded from the original 1391 particles is plotted as a function of travel distance.

4.4 Size distribution of new coarse fragments

I find that the size distributions of new coarse particles produced by fragmentation have a characteristic shape that is well-represented by a three parameter Weibull distribution, as shown in Figure 10. The Weibull distribution can be written as:

$$p(D) = \frac{\beta}{\alpha}\left(D - D_0\right)^{\beta-1} e^{-(D-D_0/\alpha)^{\beta}} \qquad [9]$$

where α and β are the scale and shape parameters respectively and D_0 is a threshold minimum particle size. For the size distribution by number of particles, for the large drum experiment, the best fit values are $\alpha = 14.2$, $\beta = 1.4$, and $D_0 = 19$ mm, the smallest size measured. This relationship can be used in predicting the PSD of fragments scaled by the initial distribution.

5.0 Field results

A fining trend in the PSD at Inyo Creek was observed covering 2 km of travel distance (Figure 11). The signal is very messy when both cross stream and longitudinal profiles PSD are combined (Figure 11a). A better signal emerges when only the longitudinal PSD is used (Figure 11b). This may occur because the cross stream profiles cover a section of the active stream, where the signal of breakdown from debris flow transport is blurred by subsequent fluvial action.

From the total station measurements, I determined Rc is 26 m, θc is 7° (Figure 13), h is 2.6 m, Δh is 1.5 m, and B is 16 m leading to an estimated velocity of 0.76 m/s using equation 7. With $S = 0.122$ and assuming $\rho_b = 1.9$ kg/m^3, equation 8 provides an estimate of 4.5 W/m^2 for the July 2013 debris flow at the field survey site.

6.0 Comparison of experimental to field results

A key goal of these experiments is to develop a method for estimating particle wear rates in the field. I chose the Inyo Creek catchment in the eastern Sierra Nevada, California to explore the extrapolation of our laboratory results because the steep bedrock slopes are sources for frequent GRAs and debris flows. The site is underlain by granodiorite, similar to the rock used in our experiments.

The abrasion rates shown in figure 11b are not solely a function of the debris flow properties. Other mechanisms of fining that can contribute to this abrasion rate include resupply of sediment from the hillslopes as well as preferential deposition of larger particles at higher elevations. These complications make the laboratory data, where no resupply or deposition occurs, essential to the understanding of particle breakdown in the field due to debris flows.

Figure 8 shows that the laboratory measurements of the mass loss coefficient, α_M, vary as a power function of unit power calculated using equation 6. Estimates for drum power are 0.03, 0.14, and 2.62 W/m^2 for the small, medium, and large drum, respectively. This trend can be extended using the field estimate of unit power, to predict a mass loss coefficient for the Inyo Creek field site of 0.13/km.

7.0 Discussion

7.1 Particle size and mass evolution

These experiments were designed to predict breakdown rates at Inyo Creek where granular rock avalanches from higher elevations evolve into debris flows with the capturing of water and the entrainment and production of fine sediment. Therefore, my experiments started without sand, silt, or clay. The production this fine sediment by abrasion and fragmentation occurred rapidly in the experimental debris flows. This has important implications for the rheologic evolution of the flow. An increase as small as 6% by mass of mud concentration causes debris flows to travel faster, have greater pore pressures, greater grain to grain friction and potential to liquefy [Iverson 2010]. In our large drum experiments, starting with an approximately uniform cobble-sized distribution, sediment less than 2 mm made up more than 11%, 4.9%, and 2.9% of the debris flow mass after 1 km of travel distance for the large, medium, and small drum, respectively (Figure 8). Sediment less than 250 microns made up more than 6% of the debris flow mass after 1 km of travel distance in the large drum (Figure 9). In contrast, in the medium-sized drum, fine sediments were only 0.05% of the total mass after the full 1 km travel distance. This indicates, for the same initial spread in the PSD, the fine sediment concentration and thus the flow rheology will evolve differently with distance traveled, depending on the intensity of particle interactions, as scaled by the rate of energy expenditure.

The patterns of particle wear measured in the three drum experiments reported here indicate that the Sternberg one-parameter exponential model for fluvial downstream fining (equations 1 and 2) can be applied to debris flows and granular rock avalanches, at least for predicting reduction in the characteristic size and mass of the bulk sediment mixture with travel distance. Moreover, the consistent trend in the mass loss coefficient with power per unit bed area (Figure 14), suggests that rates of coarse particle fining and addition of fine sediments to the fluid phase can be predicted from simple metrics of debris flow dynamics.

As shown in figure 9, the flow in the largest drum did turn into a debris flow with the crossing of the 3% fine sediment concentration threshold. The other two drums did not pass this threshold. Even though there is a transition from a GRA to a debris flow at 0.5 km of travel in the largest drum, the trends seen in figure 8 and 9 are consistent throughout the entire 1 km of travel.

7.2 Production of fragments

Use of three drums of differing sizes demonstrates how the rate of new coarse particle production by fragmentation depends on the rate of energy expenditure in the flow (Figures 10). Fragmentation rates were greatest in the 4 m drum, and negligible in the 0.2 m drum. At the field scale, unit power may be as much as an order of magnitude greater than in the large drum; fragmentation rates may be commensurately higher. This experiment shows the need for large scale laboratory experiments where fragmentation can occur. Models for predicting fragmentation rate, combined with knowledge of the characteristic size distribution of fragments produced [e.g. Le Bouteiller et al., 2011], may permit robust prediction of the contribution of fragmentation to the evolution of particle size distributions in natural debris flows. However, unlike our laboratory debris flows, PSDs in natural debris flows evolve also due to entrainment and deposition of particles along the flow path. These processes are analogous to the selective sorting and resupply by hillslopes and tributaries that complicate interpretation of downstream fining patterns in fluvial channel networks [Sklar et al., 2006].

7.3 Experimental limitations

My estimate for breakdown rates at Inyo Creek could be inaccurate for a couple reasons. Savage Number at the Inyo Creek site is ~ 0.01, roughly a third of what they are in the drums. A higher Savage Number means harder rock collisions, which would increase the production and abrasion rates. Furthermore, the PSD is wider at Inyo Creek than the PSD used in the drums. A wider distribution has the potential to increase production and abrasion rates because relatively larger particles are colliding with smaller particles. The smaller particles have a greater chance of fragmenting when they collide with a larger particle. Furthermore, a wide distribution promotes features seen in natural debris flows such as a coarse toe. The coarse toe can be influential to the flow dynamics and was not present in our study because of the narrow initial PSD.

The smallest drum has larger size abrasion coefficients than the medium drum. This could be due to the scaling of the experiment. As smaller clasts are used for the smaller drum, the ratio of the grain size to the clast b-axis becomes large. The influence of increasing pore fluid pressures has been shown to decrease with the scaling of the experimental set-up [Iverson, 2015]. This leads to a larger shear resistance, and potentially higher abrasion rates. Another result of the scaling was that I could not measure every particle in the small drum with calipers because the grains were too small. Therefore, I had to measure the weight of each grain which I then used to predict the size of the particle using an equation from a regression fit of size and weight data. Furthermore, as presented in section 4.3, where no fragmentation occurred in the smallest drum, the medium drum did produce clasts.

The experiments also reveal limitations in the exponential model. Rates of particle size reduction and mass loss are not constant, as the model assumes, but instead decline with increasing travel distance (Figures 7 & 8). Several effects may be responsible for this. First, abrasion reduces particle angularity, as initial collisions preferentially erode vulnerable high curvature surface areas. These areas must be rounded before a 2nd phase of particle size reduction starts in which the spherical gain begins loses size without changing its roundness [Domokos et al., 2014]. Second, addition of fines to the fluid increases viscosity and may dampen the intensity of particle collisions. Third, fragmentation and abrasion together reduce particle sizes and widen the particle size distribution, reducing the frequency of high energy collisions between large grains. More complex particle wear models are needed to account for these effects.

7.4 Future work

Future work in this experimental program will include validating the scaling with drum size by adding a fourth drum with a diameter of 1.2 m. This will provide data from a drum with the potential for an intermediate degree of fragmentation. This will allow for finding a relationship between fragmentation rate and power, and between fragmentation and abrasion rate. This drum will also provide a set of runs with particles large enough for caliper analysis, which can then be compared to the data in figure 7 to see if the jump in abrasion coefficients seen in the small drum is a result of the conversion from mass to size. Other future work will include investigating the sensitivity of particle wear rates to Savage Number, which can be adjusted by changing particle size and rotational velocity systematically in each wheel. Also, the influence of initial PSD will be investigated by in future experiments that vary the initial spread of the size distribution. Furthermore, an investigation is necessary to see whether these patterns hold for greater travel distances once the 2nd phase of abrasion begins [Domokos et al., 2014], which I do not believe our particles have reached yet and may never reach if fragmentation rates are high.

8.0 Conclusions

I created laboratory granular rock avalanches and debris flows in three drums with diameters ranging from 0.20 to 4 m. The flows were geometrically and dynamically similar, but had energy expenditure rates that varied over two orders of magnitude. The mass abrasion coefficient in the 0.56 and 4 m drums are within a couple percent of each other after the first 0.25 km of travel distance, but diverge significantly afterwards. The average mass abrasion rates (<250 microns) over the full kilometer of travel are .004/km, 0.005/km, 0.06/km in the 0.20 m, 0.56 m, and 4 m drums, respectively. Production of coarse fragments in the 4 m drum was an order of a magnitude larger than in the 0.56 m drum, leading to a steady decline in the abrasion coefficient for the 0.56 m drum. Fragmentation was negligible in the 0.20 m drum. The 4 m drum has a relatively high degree of fracturing and therefore maintains its high abrasion coefficient. The products from fragmentation fit well with a Weibull function. Because the Savage and Froude numbers were held constant between flows, they cannot explain the large variation in particle wear rates between drums. Instead, I propose the use of unit debris flow power to scale particle fining rates from laboratory debris flows to natural settings. Estimates for power are 0.03, 0.14, 2.62 W/m^2 in the three drums, and 4.5 W/m^2 for Inyo Creek leading to a prediction for field α_m of 0.13/km. However, we believe this estimate for field power would be improved if one includes the effects of the wider PSD and lower Savage number in the field. Therefore, further investigation is necessary to find how abrasion rates vary with the spread of the PSD and magnitude of the Savage number.

9.0 References

Bowman E.T., W.A. Take, K.L. Rait, C. Hann (2012), Physical models of rock avalanche spreading behaviour with dynamic fragmentation, *Canadian Geotechnical Journal,* 49(4): 460-476.

Brewer, P. A., and J. Lewin (1993), In-transport modification of alluvial sediment: Field evidence and laboratory experiments, *Alluvial Sedimentation*, edited by M. Marzo and C. Puigdefabregas, pp. 23-35, Black-well Sci., Oxford, U.K.

Brierley, G. J., and E. J. Hickin (1985), The downstream gradation of particle sizes in the Squamish River, British Columbia, *EarthSurf. Processes Landforms*, 10(6), 597-606.

Bunte, K., & S.R. Abt (2001), Sampling surface and subsurface particle-size distributions in wadable gravel-and cobble-bed streams for analyses in sediment transport, hydraulics, and streambed monitoring.

Chow, V. T. (1959): Open-Channel Hydraulics, McGraw-Hill, New York.

Domokos, G., D.J. , A. Á Sipos, & Á Török (2014), How river rocks round: resolving the shape-size paradox. *PloS one*, 9(2), e88657.

Hsu, L., W. E. Dietrich, and L. S. Sklar (2008), Experimental study of bedrock erosion by granular flows., J*ournal of Geophysical Research*, 113 (F02001). doi:10.1029/2007JF000778.

Hsu, L., W.E. Dietrich and L.S. Sklar (2014), Mean and fluctuating basal forces generated by granular flows: laboratory observations in a large vertically rotating drum, *Journal of Geophysical Research* – Earth Surface, doi: 10.1002/2013JF003078.

Kaitna, R., Dietrich, W. E., & Hsu, L. (2014), Surface slopes, velocity profiles and fluid pressure in coarse-grained debris flows saturated with water and mud. *Journal of Fluid Mechanics*, 741, 377-403.

Kodama, Y. (1994), Downstream changes in the lithology and grain size of fluvial gravels, the Watarase River, Japan: Evidence of the role of abrasion in downstream fining", *J. Sediment. Res.*, Sect. A, 64(1), 68-75.

Iverson, R. M., M. Logan, R. G. LaHusen, & M. Berti (2010), The perfect debris flow? Aggregated results from 28 large-scale experiments, *J. Geophys. Res.*, 115, F03005, doi: 10.1029/2009JF001514.

Iverson, R.M. (2013), Mechanics of debris flows and rock avalanches, *Handbook of Environmental Fluid Dynamics*, v. 1, H.J.S. Fernando, ed., CRC Press / Taylor & Francis, Boca Raton 573-587.

Iverson, R.M., and George, D.L., (2014), A depth-averaged debris-flow model that includes the effects of evolving dilatancy. I. physical basis,*Proceedings of the Royal Society of London*, Ser. A, 470, 20130819, doi: 10.1098/rspa.2013.0819

Iverson, R.M., (2015), Scaling and design of landslide and debris-flow experiments, *Geomorphology*, doi: 10.1016/j.geomorph. 2015.02.033.

Le Bouteiller, C., F. Naaim-Bouvet, N. Mathys, and J. Lavé (2011), A new framework for modeling sediment fining during transport with fragmentation and abrasion, *J. Geophys. Res.*, 116, F03002, doi: 10.1029/2010JF001926.

Pierson, T.C., Costa, J.E., (1987), A rheologic classification of subaerial sediment–water flows. In: Costa, J.E., Wieczorek, G.E. (Eds.), Debris Flows/Avalanches: Process, Recognition, and Mitigation, *Geological Society of America. Review Engineering Geology*, USA, pp. 1–12.

Scheidl, C., B.W. McArdell, & R. Dieter (2015), Debris-flow velocities and superelevation in a curved laboratory channel, *Can. Geotech. J.* 52: 305-317.

Schneider, D., R. Kaitna, W.E. Dietrich, L. Hsu, C. Huggel, & B.W. McArdell (2011), Frictional behavior of granular gravel–ice mixtures in vertically rotating drum experiments and implications for rock–ice avalanches, *Cold Regions Science and Technology*, 69(1), 70-90.

Sklar, L.S., W.E. Dietrich, E. Foufoula-Georgiou, B. Lashermes and D. Bellugi (2006): Do gravel-bed river size distributions record channel network structure? *Water Resources Research*, Vol. 42, No. 6, W06D18, doi:10.1029/2006wr005035.

Sternberg, H. (1875): "Untersuchungen uber Langen- und Querprofil geschiebefuhrender Fiusse: Zeitschrift fur Bauwesen." v. 25, p. 483-506.

Stock, J., & W.E. Dietrich (2003), Valley incision by debris flows: Evidence of a topographic signature, *Water Resources Research*, 39(4).

TABLES

Table 1: Experimental variables that are constant for all drums.

Rotational Froude Number, Fr	0.051
Drum width/D50-initial	7.0
Sediment depth/D50-initial	6.0
Drum width/drum radius	0.4
Total distance traveled (km)	1.0
Rock tensile strength (MPa)	7.6

Table 2: Experimental variables that differ between drums.

	Large drum	Medium drum	Small drum
Radius, r (m)	2	0.28	0.10
Width (m)	0.8	0.11	0.04
Speed, u (m/s)	1	0.37	0.23
Speed, w (rad./s)	0.5	1.34	2.22
Run time (min.)	4.2	11.1	18.5
Total time (min.)	16.7	44.6	74
D84-initial (mm)	129	20	7
D50-initial (mm)	110	17	6
D16-initial (mm)	90	14	5
Shear rate (1/s)	3.03	7.25	12.8
Savage number	0.029	0.025	0.028
Unit power (W/m2)	2.6	0.14	0.03

FIGURES

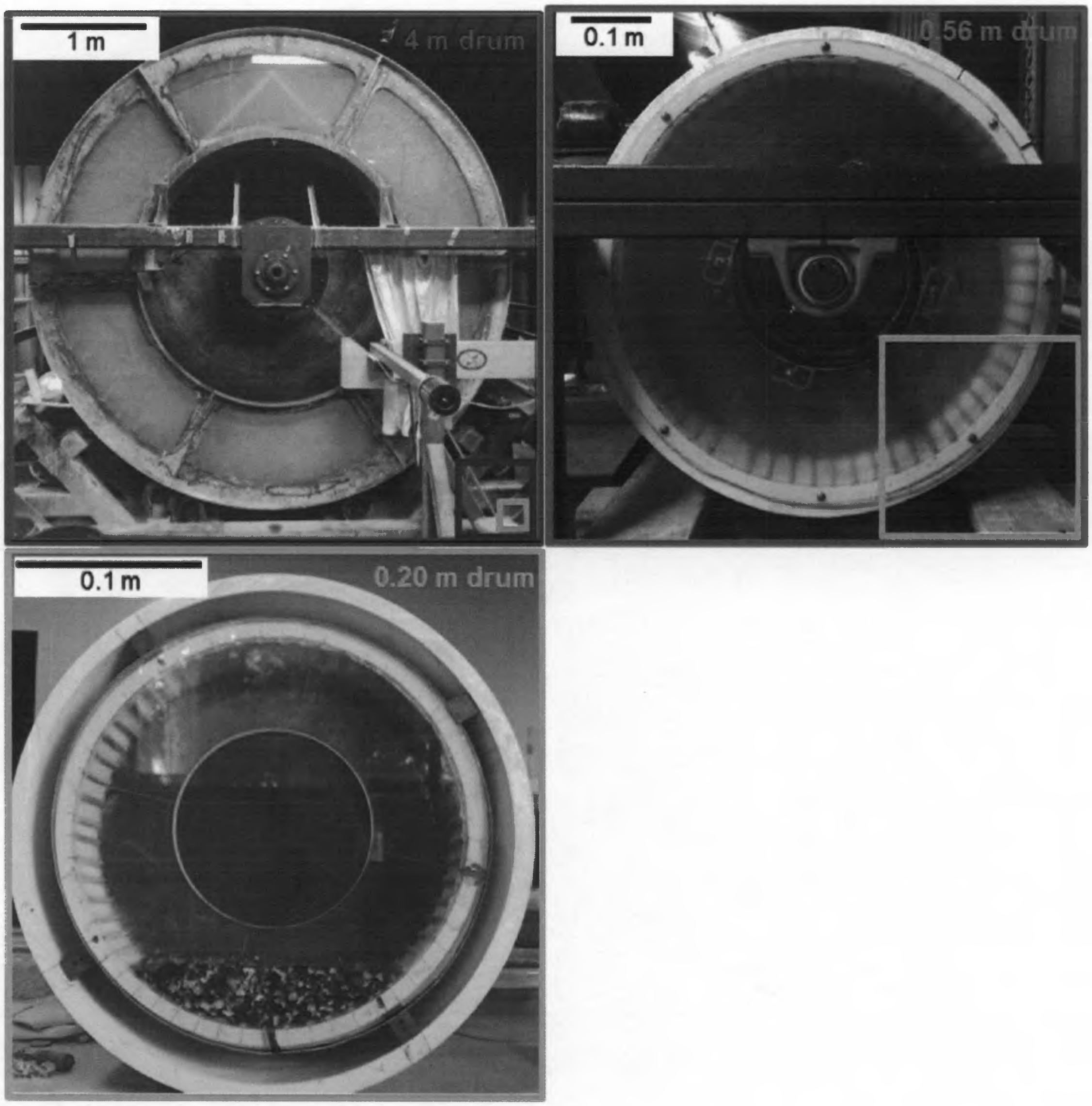

Figure 1: Top panels show the 4 m and 0.56 m diameter drum. Bottom panels show the 0.20 m diameter drum.

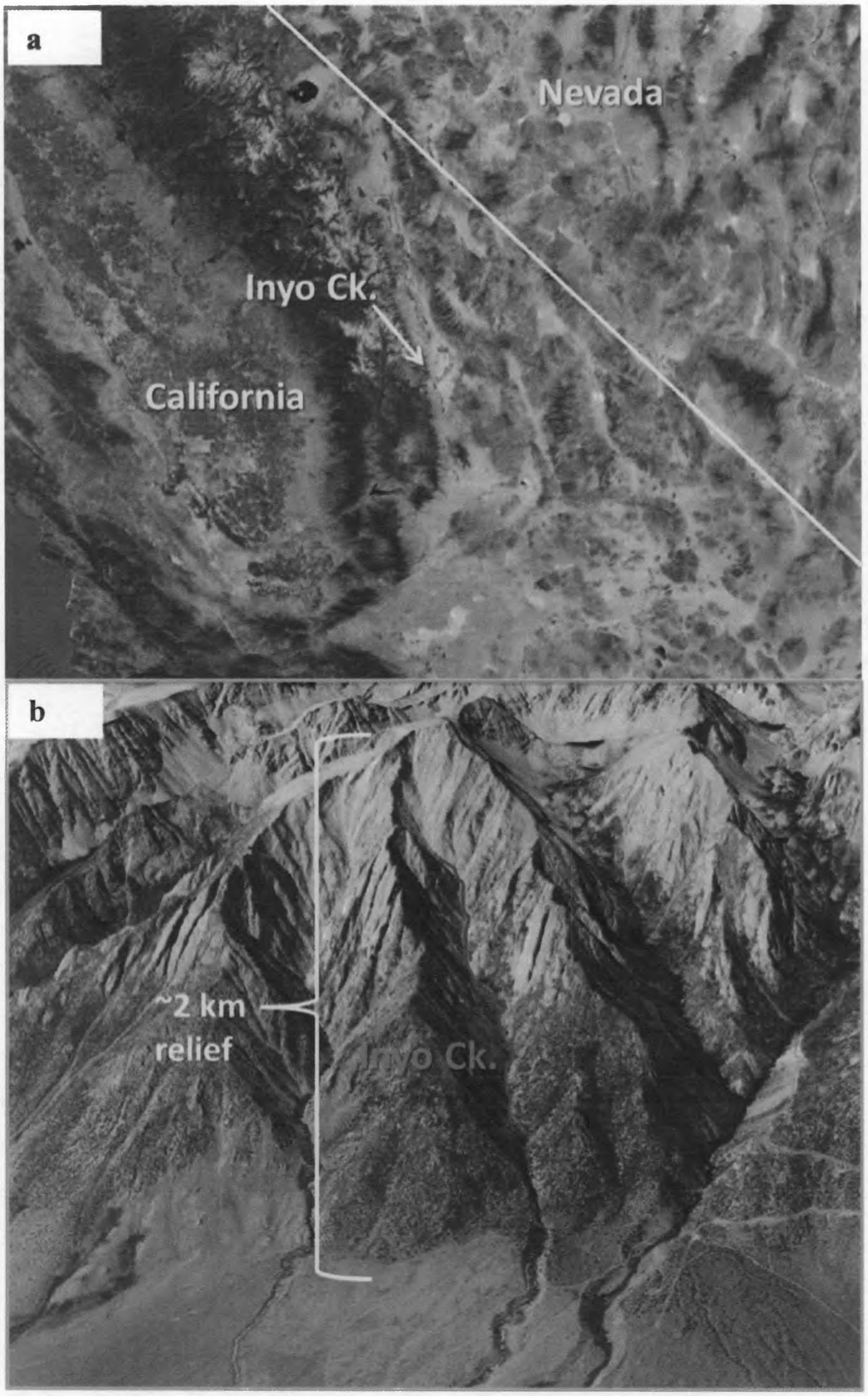

Figure 2: Panel A shows the general location of Inyo Creek, located in the southeastern Sierras. Panel B shows a GoogleEarth generated image of the drainage, which has a relief of 2 km.

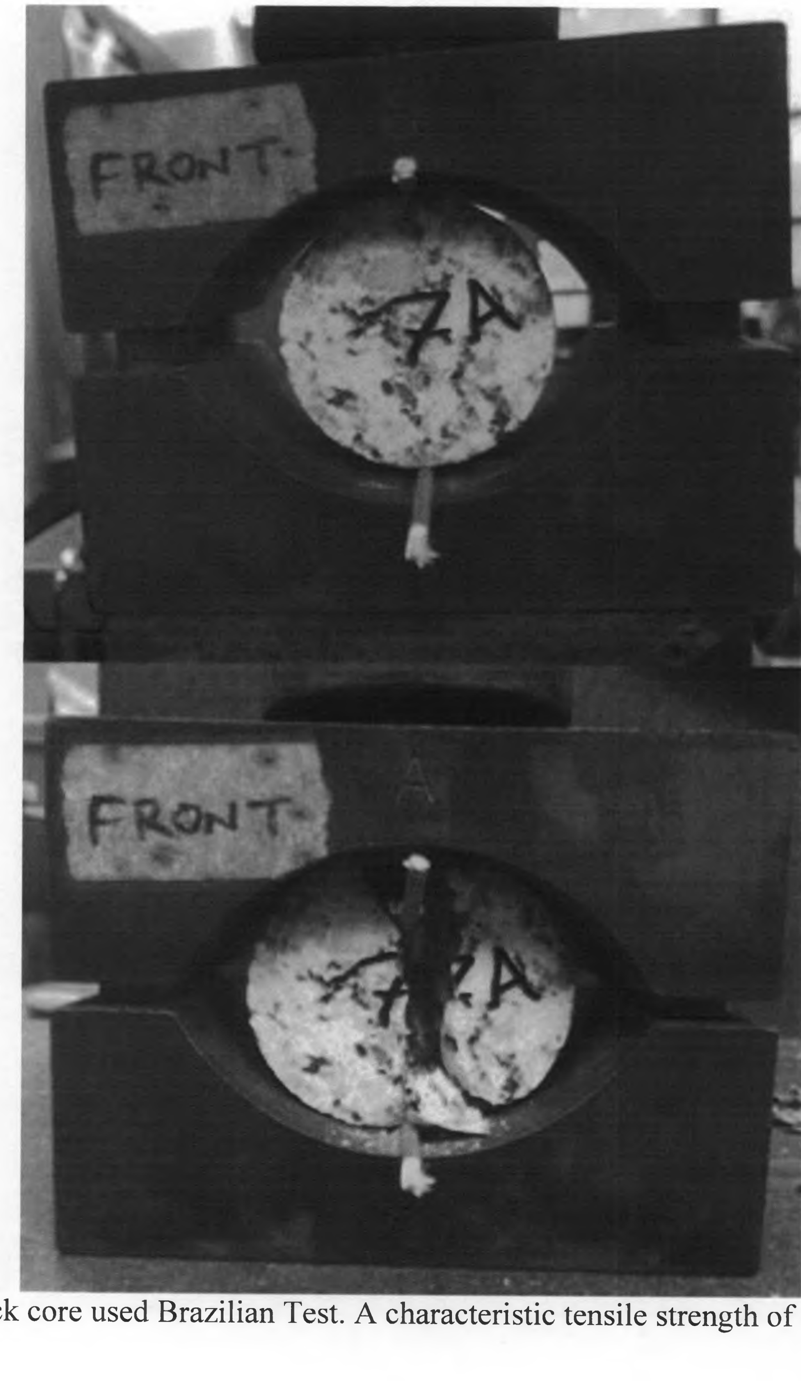

Figure 3: Rock core used Brazilian Test. A characteristic tensile strength of 7.6 MPa was found.

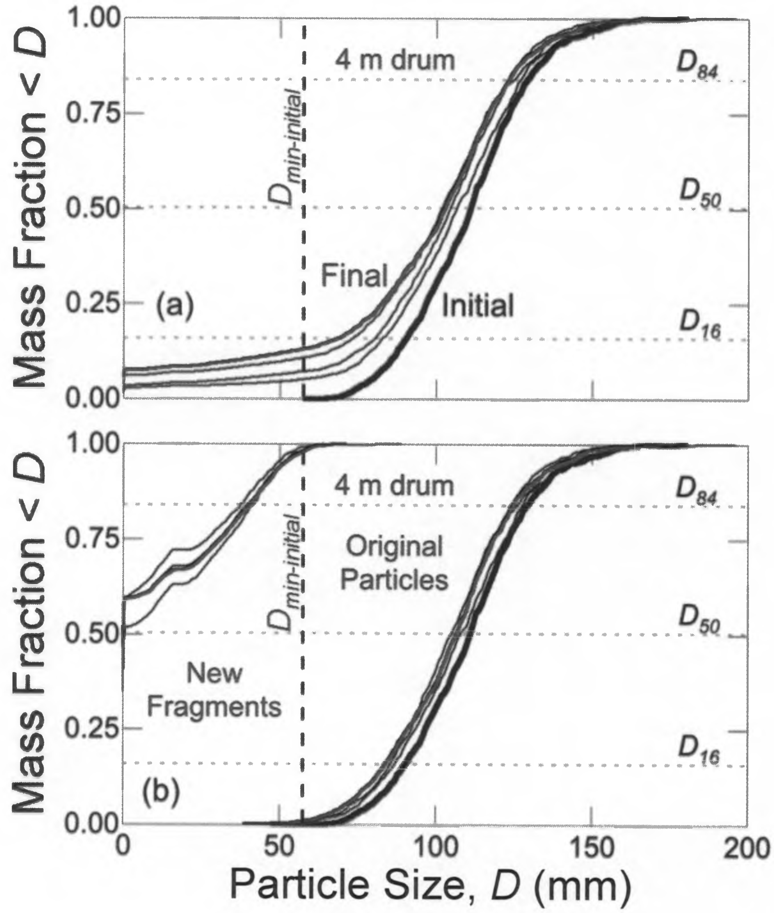

Mass Fraction < D
1.00
0.75
0.50
0.25
0.00
4 m drum
D_min-initial
Final
Initial
(a)
D84
D50
D16
4 m drum
Original Particles
New Fragments
(b)
0
50
100
150
200
Particle Size, D (mm)

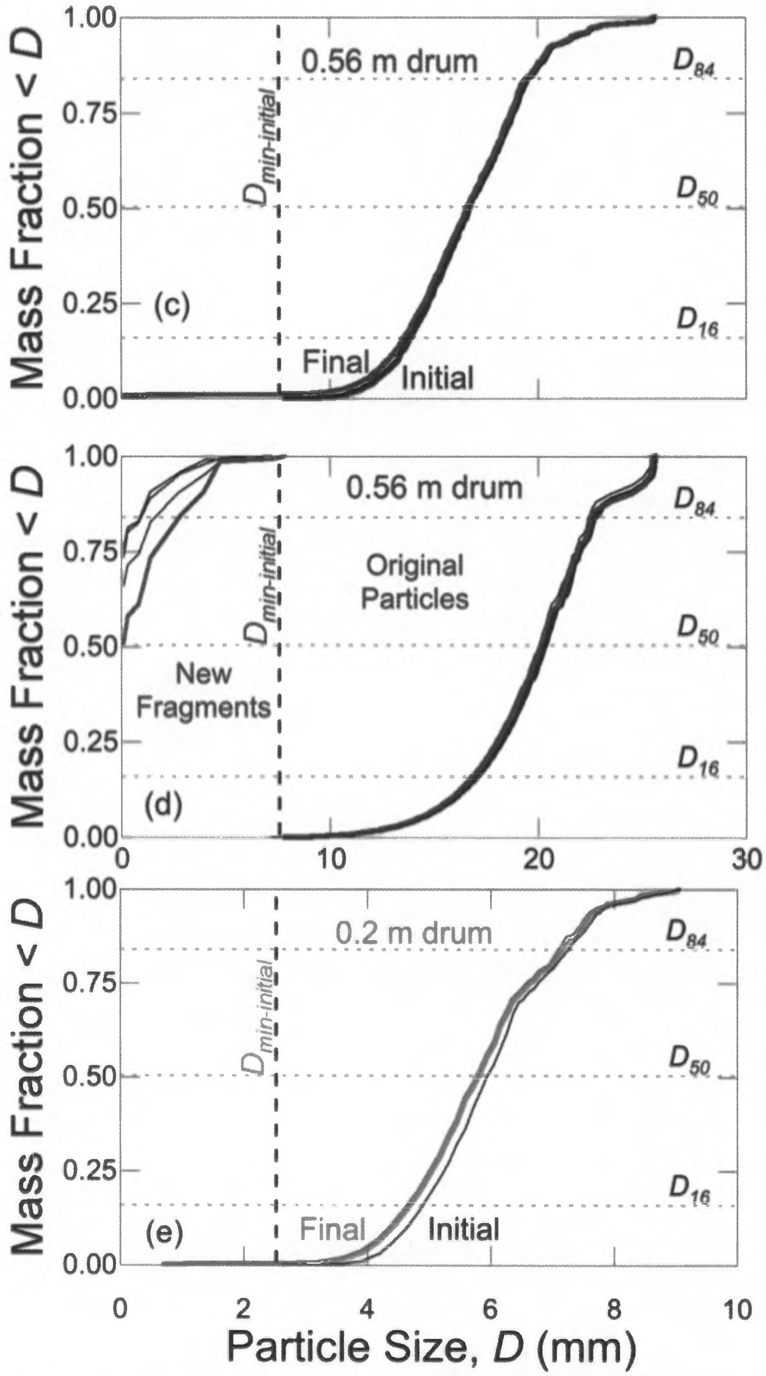

Figure 4: Panels a and b exhibit PSDs for the 4.0 m drum. Panels c and d show PSDs in the 0.56 m drum, and figure e shows the PSD in the 0.2 m drum. There is no split distribution for the 0.2 drum because no appreciable fragmentation occurred.

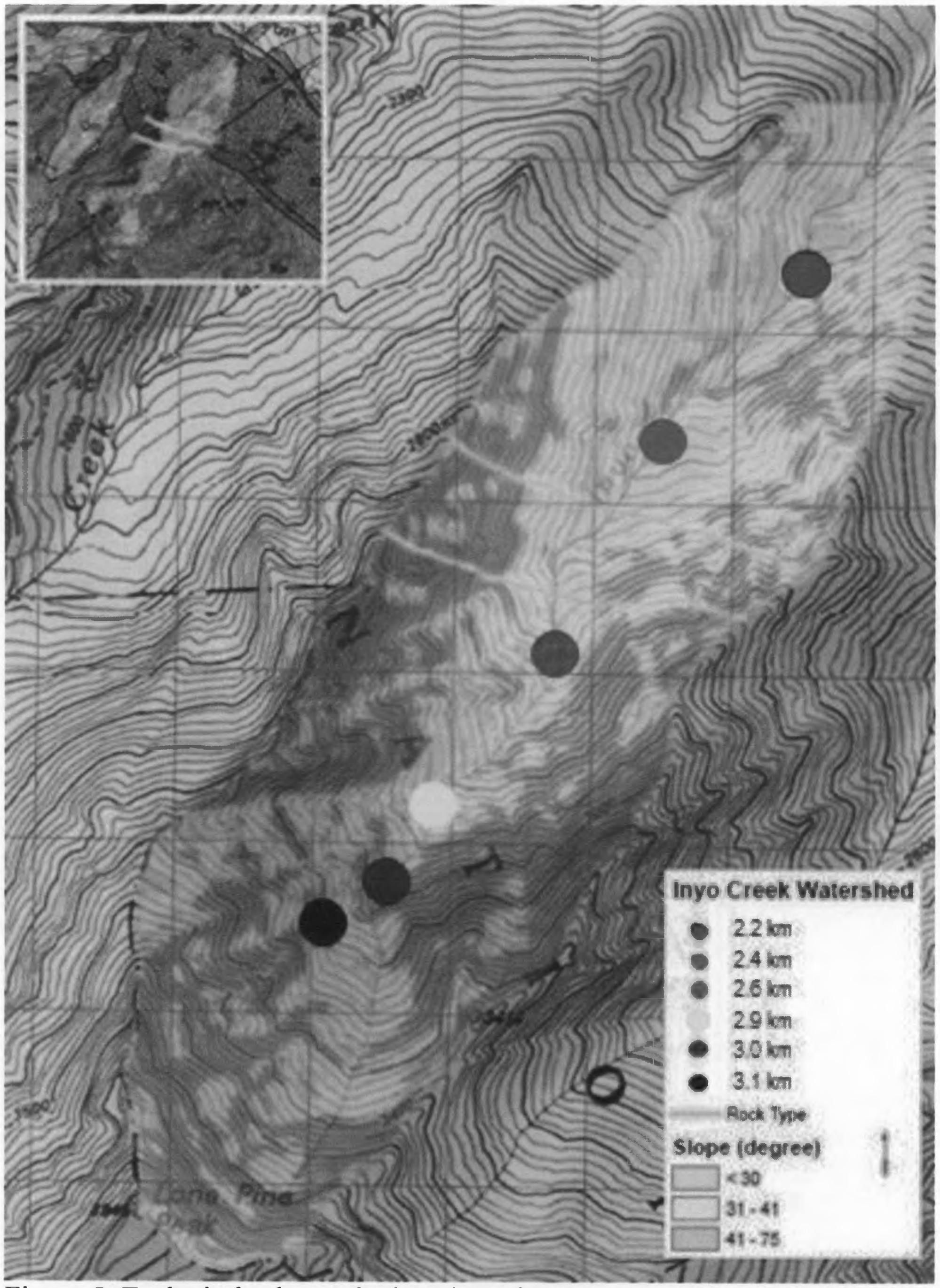

Figure 5: Each circle shows the location of the photographic pebble counts at Inyo Creek overlaid on a slope map.

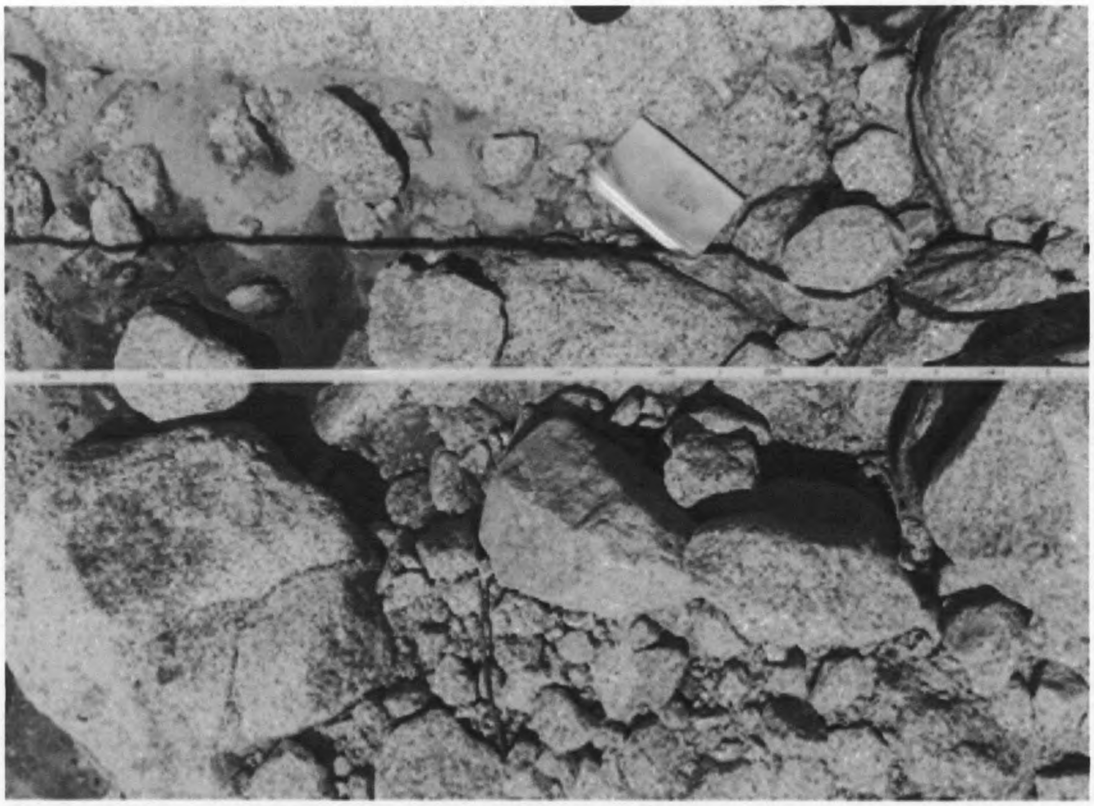

Figure 6: Example of a photograph used to get pebble counts.

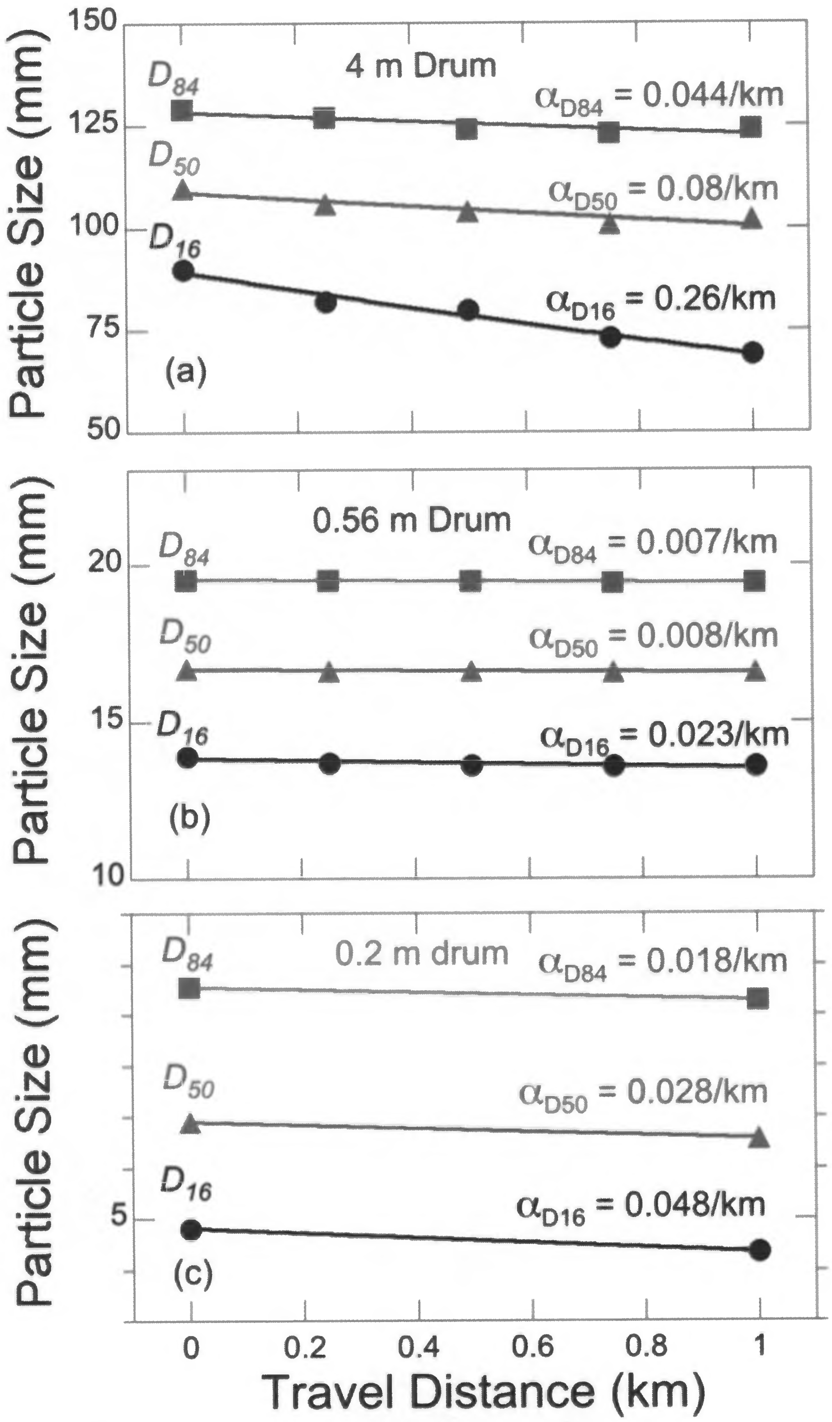

Figure 7: Evolution of size distribution percentiles.

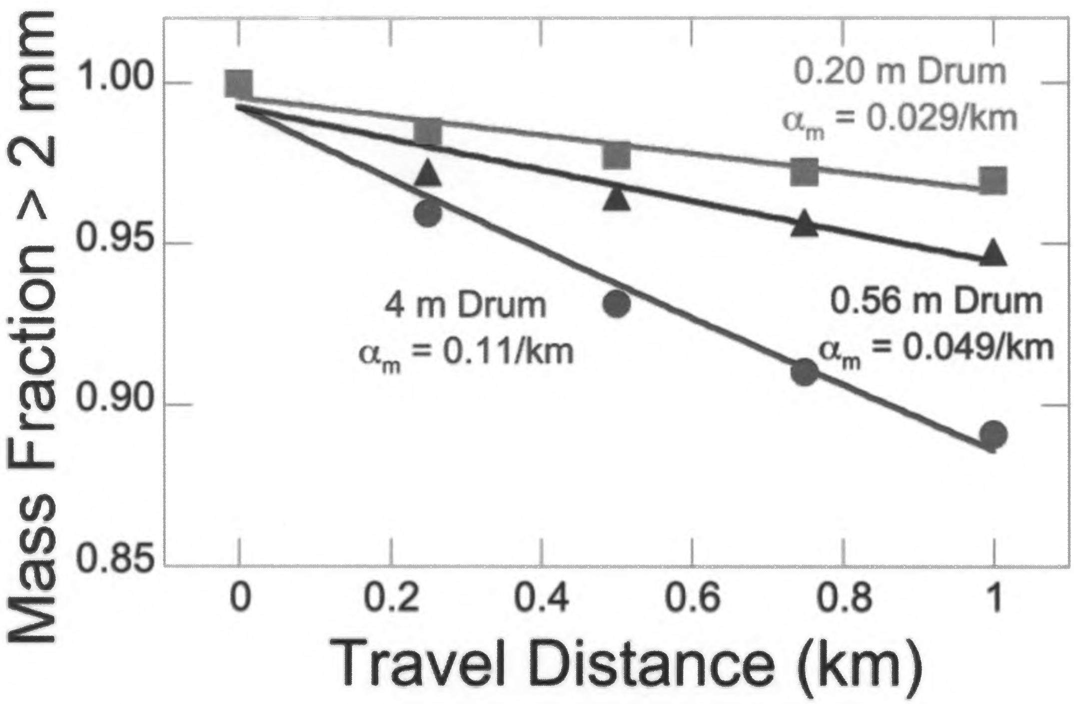

Figure 8: Mass loss from coarse size fraction to sediment less than 2 mm.

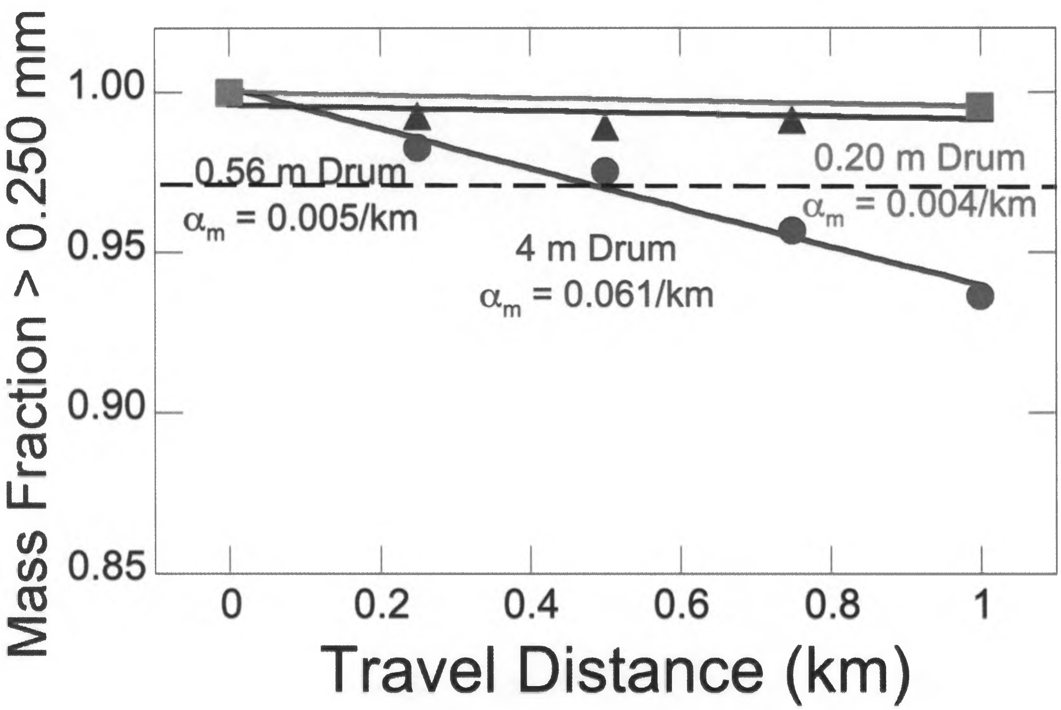

Figure 9: Mass loss from coarse size fraction to sediment less than 250 microns. The dashed line represents the 3% mud content threshold to transition from a rock avalanche to a debris flow.

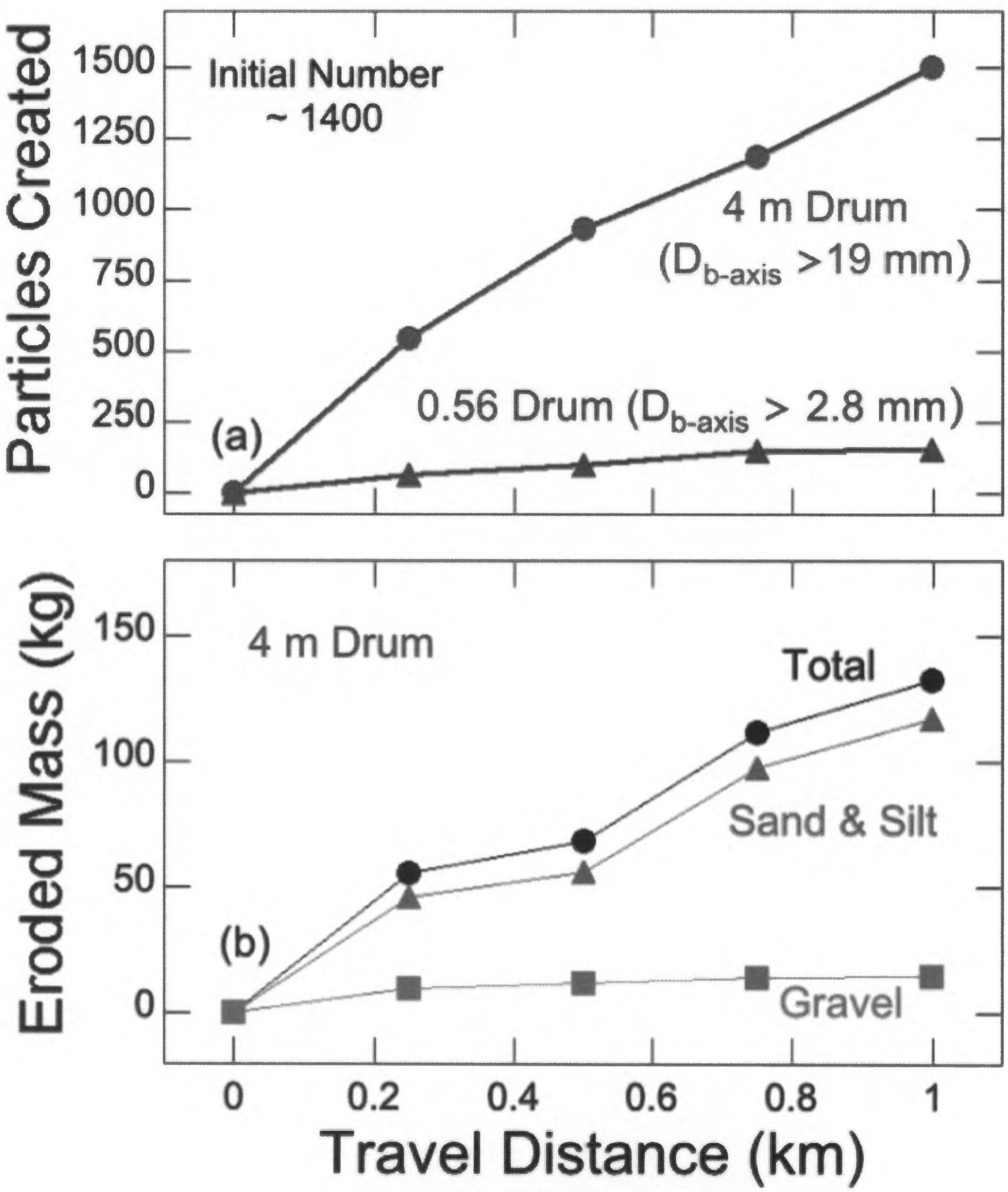

Figure 10: Production of new particles by fragmentation and abrasion. (a) Number of coarse fragments produced versus travel distance in the 4 m and 0.56 m drums. (b) The cumulative mass of new gravel, sand, and silt in the 4m drum.

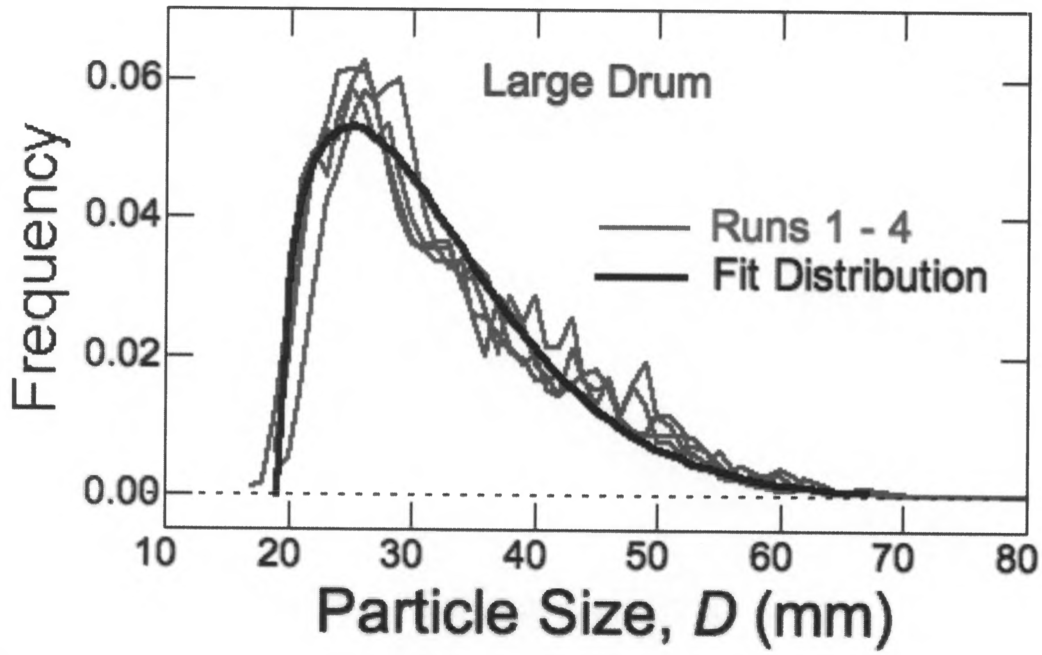

Figure 11: Distribution of new coarse fragments in 4.0 m drum.

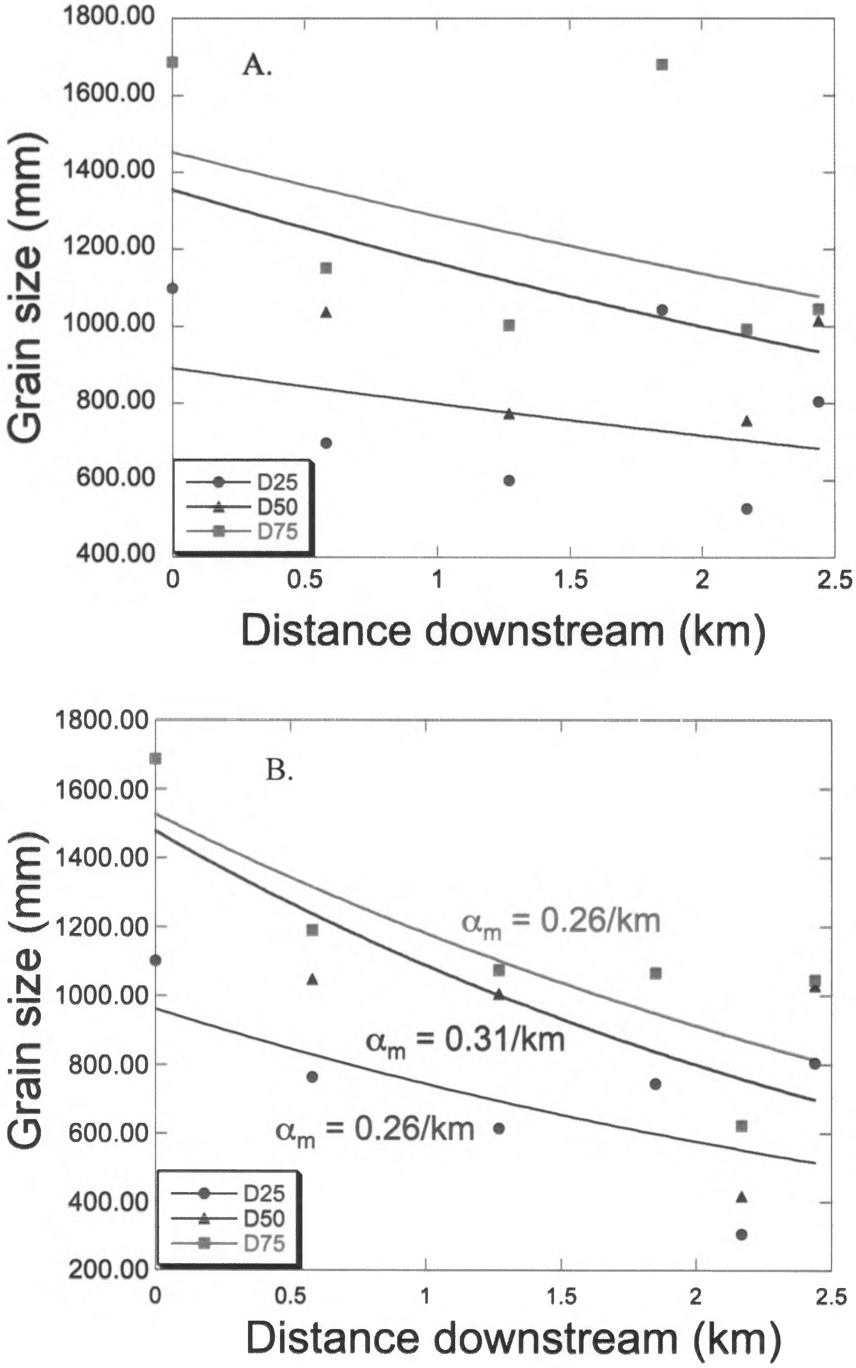

Figure 12: Results from the photographic pebble counts at Inyo Creek. Panel A shows longitudinal and cross stream profiles combined. Panel B only shows the longitudinal profile data.

Figure 13: Field survey of debris flow track at Inyo Creek, CA, with the terms in the super-elevation calculation annotated.

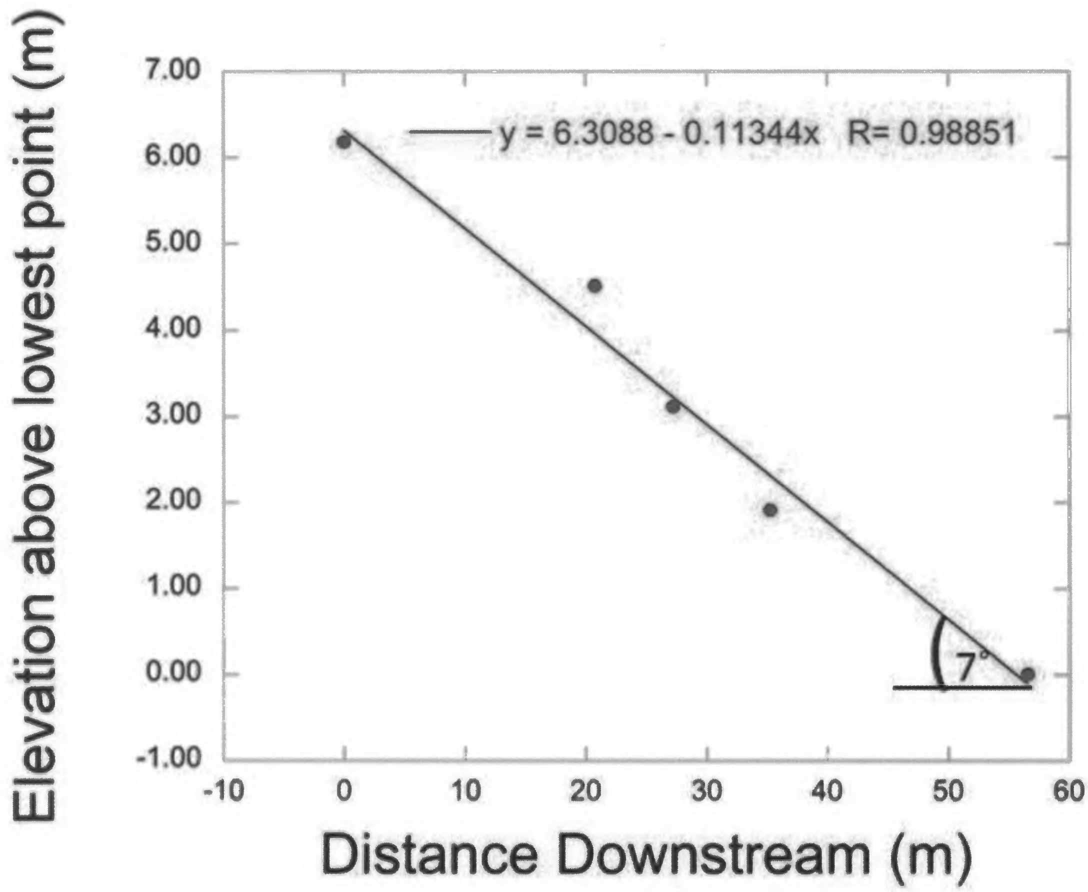

Figure 14: Each point represents the midpoint of each cross section taken with the total station at Inyo Creek. Connecting these midpoints with a line provides a good estimate for the slope the debris flow experienced going around the bend.

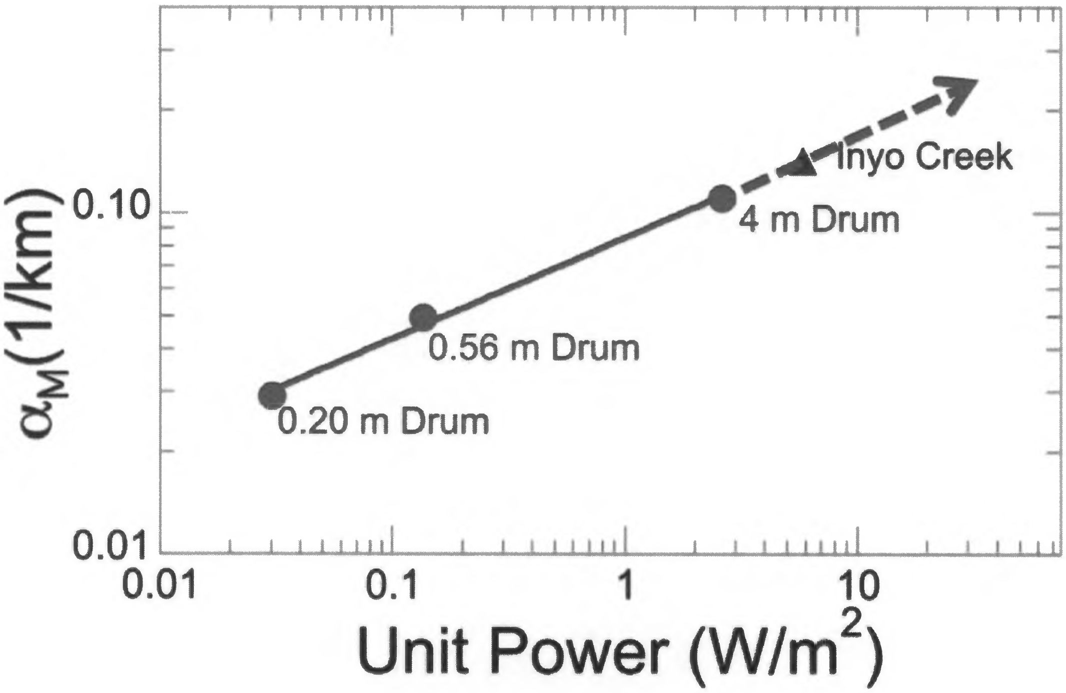

Figure 15: Extrapolation of laboratory mass loss coefficients to field conditions at Inyo Creek, CA, using an estimate of unit power.